# Optical properties of aerosols measured by Lidar, Sun-photometer, and other ground based instruments

**J. B. Nee and C. W. Chiang**

*Department of Physics, National Central University, Chung-Li, Taiwan,*

*jbnee@phy.ncu.edu.tw; cwchiang@alumni.ncu.edu.tw*

**ABSTRACT:**

By using Lidar, Sun-photometer, and other ground based instruments characteristics of aerosols in 0-5 km at Chung-Li (25°N, 121°E) are investigated. The optical thickness, or atmospheric extinctions, in 0-5 km show seasonal variation resulting from different aerosol sources, the mechanism of long range transport, and local atmospheric environment. Overall, 75% of atmospheric extinction is contributed by the aerosols in the boundary layer (BL), and about 20% from the height region of 1 to 3 km, the remaining extinction is caused by upper level aerosols, Sources of aerosols including desert dust, biomass burning, and local air pollution are identified from the satellite imageries, back trajectory calculations, and chemical and particulate measurements Their respective optical properties in terms of Lidar backscattering ratio and depolarization ratio are plotted and identified.

## 1. INTRODUCTION:

Aerosols are now widely monitored by using various instruments to determine their effects on environment and climate. Sun-photometer has been versatile in measuring the optical thickness through the column air. Chemical and particulate measurements are useful in determine their chemical properties. Lidar technologies can provide not only the vertical distribution, but also optical and microphysical properties. We have used these combined data at Chung-Li, Taiwan (25°N, 121°E) to measure aerosols in the lower atmosphere over the years. Several important aerosols sources including sea salt, dust storm, local pollution and biomass aerosols are identified.

The largest atmospheric extinction is related to aerosols is in the region of boundary layer. Aerosols are not only responsible for the extinction, they can also show properties of the boundary layer. For example, turbulence, convective activities, wind and waves are also important properties in the BL and all can be investigated by using aerosol scattering.

## 2. MEASUREMENTS OF VARIOUS INSTRUMENTS:

### 2.1 Lidar system:

The Lidar provides the best data for aerosols in 0.5-5 km. The backscattering coefficient and depolarization ratio are measured. Calculations were made based on Klett's algorithm [1,4].

### 2.2 Sun-photometer:

The AERONET sun-photometer is also located at Chung-Li. The Aerosol Optical Thickness (AOT) and the aerosol size distribution (ASD) can be determined from sun-photometer measurements. In the present study, AOT is determined by data at 440 and 670 nm which have been interpolated to obtain the equivalent AOT at 532 nm.

**2.3 Visibility/Visual distance (VD):**

In the ground level between 0-1 km, lidar signals were poorly measured in our setup, particularly below 0.5 km. We have used the visibility data from a nearby airport to provide extinction data in 0-1 km. The volume extinction coefficient can be derived from visibility data through the Koschmeider relationship given as $VD = \mathbf{3.91}/k$ ($k$ is the extinction coefficient) [2] by assuming the homogeneous atmosphere in the region of 0-1 km. Combined lidar, sun-photomer, and visibility measurements provided us with optical properties of the atmosphere from 0 km up as shown in Fig.1. We found from Fig.1 that AOT in the height region 1-3 km is about 20-25% of the total column, with the rest mainly contributed by air below1 km.

**2.4 $PM_{10}$ and chemical measurements:**

Local EPA station provide the particulate measurements and several stations have data on chemical analyses. Their results of elemental compound during various dust storm period are useful to understand properties of aerosols. Results in Taipei, a northern city of Taiwan showed increased sea salt and pollutants for dust days compared with non-dust days. For example, elevated concentrations of $Na^+$, $K^+$, $Mg^{2+}$, $Ca^{2+}$, and $Cl^-$ were found in the fine mode particles and enhanced $Na^+$, $Mg^{2+}$, $Ca^{2+}$, $NO_3^-$, and $SO_4^{2-}$ in the coarse mode particles [3]. The fine mode particles were believed to be related with local pollutions while the coarse mode particles were from transported dust. On average, sea salt indicated by $Na^+$ and $Cl^-$ in the coarse mode showed an increase by a factor of two to four during dust period, and the pollutants, such as $NO_3^-$ and $SO_4^{2-}$ compounds, increased by a factor of two [3,5]. Elements of Fe, Si, Ti were also increased during dust events.

**3 Aerosol distribution and seasonal variation:**

The height profiles for aerosols are averaged for 2002-2004 in terms of the (a) backscattering ratio and (b) accumulated extinction coefficient for all seasons as shown in Fig.2. We found that the majority loading of aerosols lies in the height region 1-5 km in the spring, and below about 1 km the summer time aerosol dominates. The seasonal dependence of aerosol loading may be understood in terms of their sources, transportation mechanism, and local weather conditions. Analyses of Radiosonde data for wind speed show spring time aerosols are transported by wind at 1-3 km region. Their sources can be found by using the back trajectory calculations and TOMS aerosol index (AI). It is quite evident that springtime aerosols are dominated by Asian dust produced in the northern China and the biomass burning aerosols from Southeast Asia. Their long range transport result local aerosols from Southeast Asia dominate in the upper air in 2-4 km, whereas dust aerosols were found below 2 km.

The Asian dust normally transport to the east through weather system. However, winter northeasterly monsoon will sometimes bring dust southward to the East China Sea by the Asian continental outflow. The result is the transport of dust to the southern Asian including Taiwan.

**4. Optical properties of various types of aerosols:**

Lidar backscattering and depolarization ratios are plotted to show characterization of aerosols. Fig.3 shows various aerosols have their distribution region in the plot. For example, the distribution of backscattering and depolarization ratios of biomass aerosols are scattered, but seem to be mainly located in the upper region of the graph with the largest backscattering and depolarization ratios. The pollutant lies in the lowest region of the graph with

smallest depolarization ratios; and the dust events seem to locate in-between. The solid symbols indicate the events verified by ground base particulate measurements of EPA and also confirmed with TOMS images.

**5. Particle Size distributions:**

The particle average size distribution **(**ASD) is related with the scattering phase function, single scattering albedo, and the spectral variation of AOT. AERONET has been used in the present study. In Fig. 4, the particle size distributions of background aerosols in the months of March of the 2002 and 2003 are calculated (solid diamond curve), the vertical bars represent the standard deviation magnitude of the accumulation mode $\frac{dV}{d(\ln r)}$. The background aerosol (solid diamond curve) indicates a bimodal size distribution with two mode radius of 0.2 $\mu m$ and 2 $\mu m$ respectively. The column size distributions of the biomass event (circle curve) and Asian dust storm event (triangle curve) on 22 March 2002 and 24 January 2003 respectively are also presented. The biomass aerosols show largest sizes. Dust particles are dominated by fine mode. These events were also observed by Lidar. The volume size distributions display a significant differences among background aerosols, dust and biomass in the portion of fine mode ( 0.4-0.7 $\mu m$ ) and coarse particles ( > 5 $\mu m$ ).

**FIGURES:**

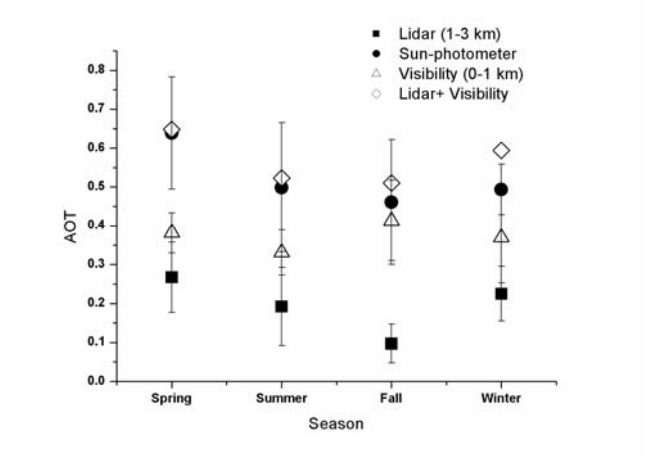


Fig. 1. The optical depth derived by lidar, sun photometer and visibility.

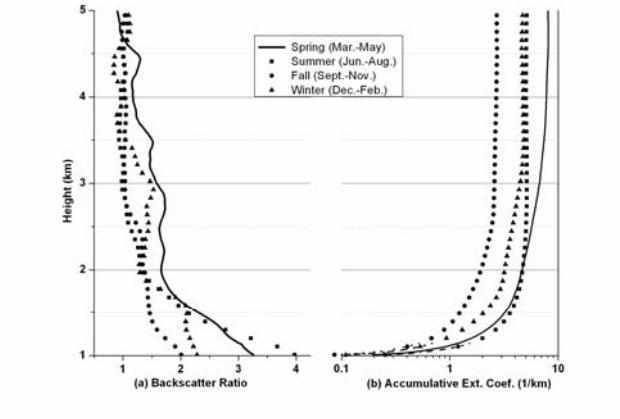


Fig. 2. (a) aerosol backscattering ratio and (b) accumulative extinction coefficient.

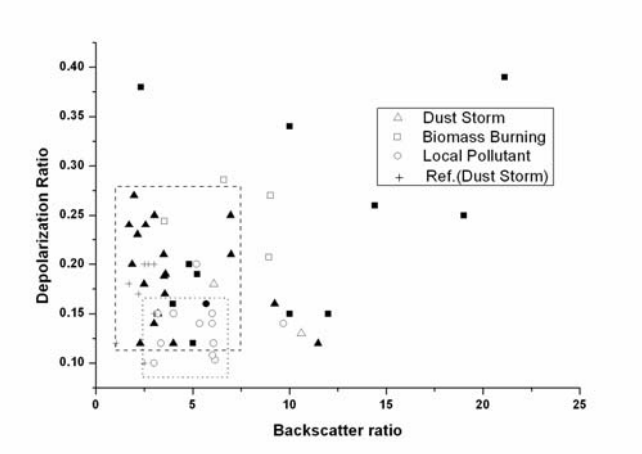


Fig. 3. Summarizing the type of aerosols. The solid symbols indicate the events verified by EPA and TOMS. Ref. (cross symbols) are the results of dust observation from literatures.

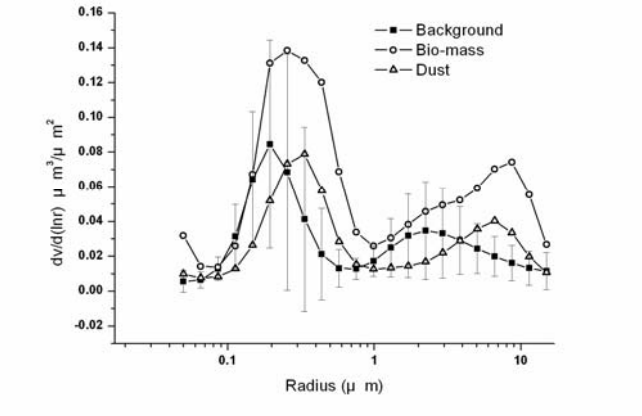


Fig. 4. The profiles of column size distribution of background aerosol, dust event and biomass burning event.

**REFERENCE:**

1. Chen, W.N., et al., Lidar ratio and depolarization ratio for cirrus clouds, *Appl. Opt*., 41, 6470-6476, 2002.

2. Griffing, G.W., Relations between the prevailing visibility, nephelometer scattering coefficient and sunphotometer turbidity coefficient, *Atmos. Environ.*, 14, 577-584, 1980.

3. Lung, S.C., et al., Water-soluble ions of aerosols in Taipei in spring 2002, *TAO*, 15, 901-923, 2004.

4. Nee, J.B., et al., Lidar detection of cirrus cloud in Chung-Li (24.96°N, 121.19°E), *J. Atmos. Sci*. 55, 2249-2257, 1998.

5. Yuan, C.S.,Mass concentration and size-resolved chemical composition of atmospheric aerosol sampled at the Pescadores islands during Asian dust storm periods in the years of 2001 and 2002, *TAO*, 15, 857-879, 2004.